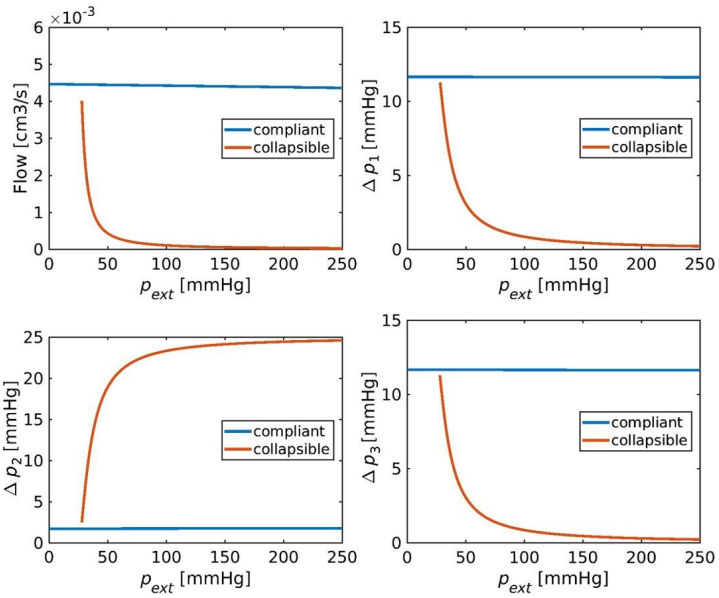

FIGURE 15.6

Top panel: fluid flow Q_v (left panel), pressure drop $\Delta p_1 = p_{in} - p_2$ (right panel). Bottom panel: pressure drop $\Delta p_2 = p_2 - p_4$ (left panel), pressure drop $\Delta p_3 = p_4 - p_{out}$ (right panel). The graphs are the solutions of system (15.63) obtained by varying the external pressure p_{ext} in the interval $[0, 250]$ mmHg with $p_{in} = 40$ mmHg and $p_{out} = 15$ mmHg. The blue lines (dark gray in print version) report the solutions when all three compartments are modeled with a compliant hydraulic resistance whereas the red lines (light gray in print version) refer to the case in which $comp2$ is modeled as a collapsible fluid tube.

the hydraulic circuit, increases much faster: this behavior expresses the physical fact that the tube is collapsing with the increase of the external pressure.

15.7 EXAMPLE: REPRESENTATIVE SEGMENT MODEL OF THE RETINAL MICROCIRCULATION

In this section, we use the electric hydraulic analogy to model blood flow dynamics in the retina microcirculation, referring to the articles [13] and [66] and to the bibliography cited therein for more information on the physiological and biophysical aspects of the problem. Fig. 15.8 reports an image of the retinal vasculature obtained via retinal oximetry (see [135] and [322]).

Following [13] and [66], the retinal microcirculation can be divided in several segments, or compartments, by the procedure illustrated below. The vascular network, denoted by $\mathcal{N}$, is represented as a collection of cylindrical straight tubes having different diameters. We assume that:

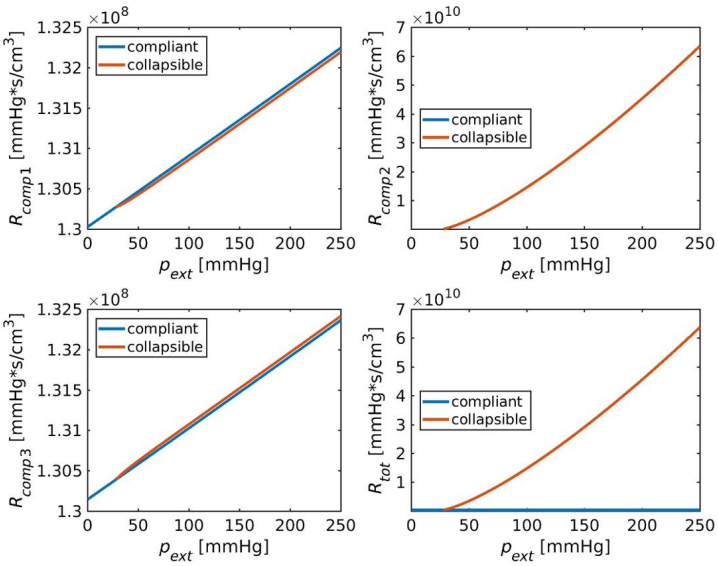

FIGURE 15.7

Top panel: $comp1$ resistance R_{comp1} (left panel), $comp2$ resistance R_{comp2} (right panel). Bottom panel: $comp3$ resistance R_{comp3} (left panel), total hydraulic resistance R_{tot} (right panel). Resistance of the three fluid compartments R_{comp1}, R_{comp2} and R_{comp3} The graphs are the solutions of system (15.63) obtained by varying the external pressure p_{ext} in the interval $[0, 250]$ mmHg with $p_{in} = 40$ mmHg and $p_{out} = 15$ mmHg. The blue line (dark gray in print version) reports the solution when all the three compartments are modeled with compliant hydraulic resistance whereas the red lines (light gray in print version) refer to the case in which $comp2$ is a collapsible fluid tube.

- $\mathcal{N}$ is subdivided into five subsets $\mathcal{V}_i$, $i = 1, \ldots, 5$, corresponding to large arterioles (LA), small arterioles (SA), capillaries (C), small venules (SV), and large venules (LV), as in [13], so that $\mathcal{N} = \cup_{i=1}^{5} \mathcal{V}_i$;
- each vessel in $\mathcal{V}_i$, $i = 1, \ldots, 5$, has the same geometric, rheological, and mechanical properties as every other vessel belonging to $\mathcal{V}_i$;
- axial symmetry holds for each vessel in $\mathcal{N}$ in such a way that every variable defined on $\mathcal{N}$ depends on the radial and axial coordinates of each vessel, denoted by r and z, respectively, and on the time coordinate t;
- the diameter of all blood vessels are assumed to be constant in time, thereby implying that resistances and capacitances are given constants.

Based on the above assumptions, we perform the *geometric model reduction* by replacing the vascular network $\mathcal{N}$ with the representative segment model $\mathcal{R}$ shown in Fig. 15.9.

Comparing the scheme of Fig. 15.9 with that in Fig. 15.8, we conclude that the set of nodes connecting the various vessels in the original network $\mathcal{N}$ (occupying well-identified spatial positions depending on the topological organization of the vessels) corresponds to a new set of nodes connecting each compartment of $\mathcal{R}$ with the neighbors, with the convention that the LA compartment is connected (on the

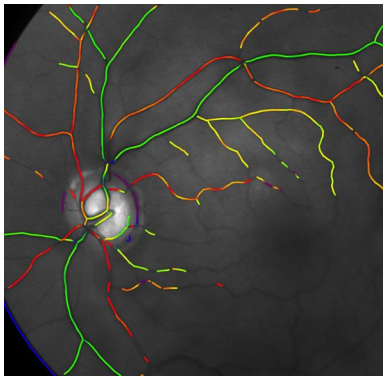

FIGURE 15.8

Retinal microcirculation network obtained via retinal oximetry (see [135] and [322]).

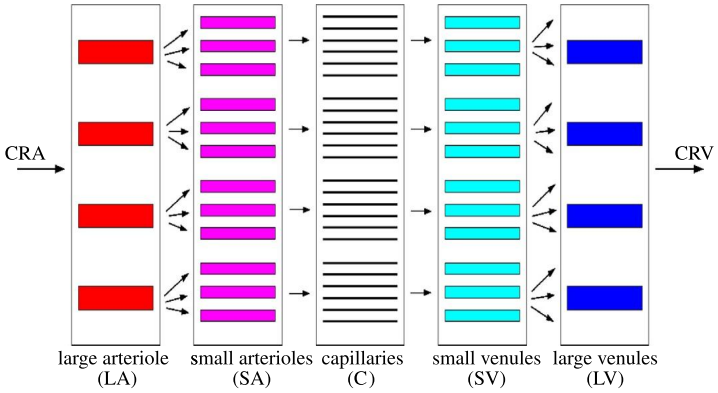

FIGURE 15.9

Representative segment model of the retinal vasculature. The picture gives a schematic view of the five principal compartments into which the retinal vessel system is divided. From left to right: the central retinal artery (CRA) branches into four main large arterioles (LA). These latter branch into small arterioles (SA), which, in turn, divide into a fine network of capillaries (C) that mediate the blood exchange between arteries and veins. The mirror structure on the right comprises small venules (SV) and four main large venules (LV) that converge into the central retinal vein (CRV), which drains the retina.

left side) to an input source node associated with the outlet of the central retina artery (CRA) and the LV compartment is connected (on the right side) to an output source node associated with the inlet of the central retina vein (CRV). We associate with each compartment of $\mathcal{R}$ an electric equivalent representation through resistive elements, whose resistance is denoted by R, and capacitive elements, whose capacitance is denoted by C, as shown in Fig. 15.10. The parameter R expresses the resistance

to blood flow in the vessel due to blood viscosity, whereas the parameter C expresses the ability of a blood vessel to deform and store blood volume.

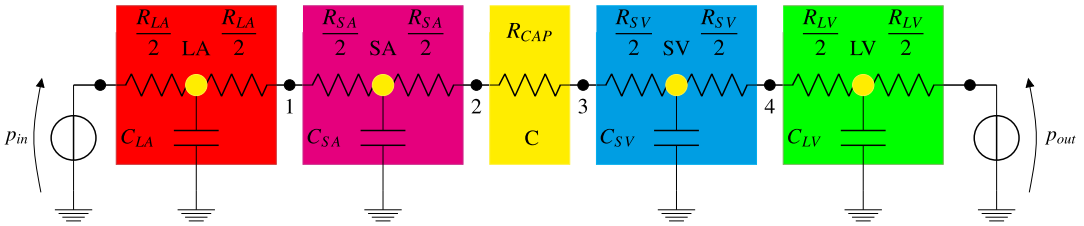

FIGURE 15.10

Schematic representation of the network model for retinal microcirculation divided in five branches: the large arterioles (LA) and small arterioles (SA), the large venules (LV) and small venules (SV), and the capillaries (C). The black bullets, numbered between 1 and 4, and the yellow bullets (light gray in print version), labeled LA, SA, SV, and LV, are the nodes of the circuit.

Proceeding as in Section 15.6, the differential model describing retinal microcirculation is given by the following set of equations:

$$\underline{\underline{\mathbf{C}}}\frac{d\underline{\mathbf{P}}(t)}{dt} = -\underline{\underline{\mathbf{Y}}}\underline{\mathbf{P}}(t) + \underline{\mathbf{I}}(t), \qquad t > 0, \tag{15.72a}$$

$$\underline{\mathbf{P}}(0) = \underline{\mathbf{P}}^0. \tag{15.72b}$$

System (15.72) results from the application of the KCL at nodes LA, SA, SV, and LV of the electric circuit of Fig. 15.10. Thus, the column vector of the nodal blood pressures is

$$\underline{\mathbf{P}} = [p_{LA}(t), p_{SA}(t), p_{SV}(t), p_{LV}(t)]^T \in \mathbb{R}^{4\times 1}, \tag{15.73}$$

the initial datum for the nodal pressures is the column vector

$$\underline{\mathbf{P}}^0 = [p^0_{LA}, p^0_{SA}, p^0_{SV}, p^0_{LV}]^T \in \mathbb{R}^{4\times 1}, \tag{15.74}$$

and the column vector of given input and output currents is

$$\underline{\mathbf{I}} = [G_1 p_{in}(t), 0, 0, G_5 p_{out}(t)]^T \in \mathbb{R}^{4\times 1}; \tag{15.75}$$

$\underline{\underline{\mathbf{C}}} \in \mathbb{R}^{4\times 4}$ is a diagonal matrix whose nonzero positive entries are the time-invariant capacitances C_{LA}, C_{SA}, C_{SV}, and C_{LV}, whereas $\underline{\underline{\mathbf{Y}}} \in \mathbb{R}^{4\times 4}$ is the symmetric positive definite admittance matrix

$$\underline{\underline{\mathbf{Y}}} = \begin{bmatrix} (G_1+G_2) & -G_2 & 0 & 0 \\ -G_2 & (G_2+G_3) & -G_3 & 0 \\ 0 & -G_3 & (G_3+G_4) & -G_4 \\ 0 & 0 & -G_4 & (G_4+G_5) \end{bmatrix}, \tag{15.76}$$

having set

$$G_1 := \left(\frac{R_{LA}}{2}\right)^{-1},$$
$$G_2 := \left(\frac{R_{LA}+R_{SA}}{2}\right)^{-1},$$
$$G_3 := \left(\frac{R_{SA}+R_{SV}}{2}+R_{CAP}\right)^{-1},$$
$$G_4 := \left(\frac{R_{SV}+R_{LV}}{2}\right)^{-1},$$
$$G_5 := \left(\frac{R_{LV}}{2}\right)^{-1}.$$

The pressures at nodes 1, 2, 3, and 4 in Fig. 15.10 can be computed by postprocessing through application of the Ohm law (15.77b) once the nodal pressures at nodes LA, SA, LV, and SV are available. The input and output pressures are denoted by p_{in} and p_{out}, respectively, and contribute to the vector $\mathbf{I}$ in (15.75); these pressures are assumed to be given functions of time and express the interaction of the vessel with the neighboring environment. Resistances R_j, for j =LA, SA, CAP, SV, and LV, are computed by assuming that the considered fluid compartment is constituted by n vessels in parallel (as depicted in Fig. 15.9). Thus, resistance to blood flow can be computed by applying the Poiseuille law (15.16), i.e.,

$$R_j = \frac{128 L_j \mu_j}{\pi n_j D_j^4}, \tag{15.77a}$$

where μ_j is the viscosity of blood flowing in a cylindrical tube of diameter D_j and length L_j within the vascular compartment j. Using the analogy between electric potential and blood pressure and between the electric current and volumetric blood flow rate, we can write the fluid dynamical equivalent of Ohm's law as

$$Q_j = G_j \Delta p_j, \tag{15.77b}$$

where Q_j is the flow rate through the jth compartment, Δp_j is the pressure drop across the compartment, and $G_j := R_j^{-1}$ is the hydraulic conductance. More precisely, the pressure drops across the compartments are defined as $\Delta p_{LA} = p_{in} - p_{LA}$, $\Delta p_{SA} = p_{LA} - p_{SA}$, $\Delta p_{CAP} = \Delta p_{SV} = p_{SA} - p_{SV}$, and $\Delta p_{LV} = p_{SV} - p_{LV}$. Following [137], we compute each capacitance C_j, for j = LA, SA, SV, and LV, as

$$C_j = \pi \left(\frac{D_j}{2}\right)^2 L_j \sigma_j, \tag{15.77c}$$

where σ_j is the vascular distensibility of the jth vascular compartment.

Table 15.2 contains the baseline values of the input and output pressures, as determined in [13,137].

Table 15.2 Baseline values of the input pressure sources.

Symbol	Description	Value	Source
$p_{in,b}$	Inlet pressure for the retinal vasculature	40 mmHg	[13,137]
$p_{out,b}$	Outlet pressure for the retinal vasculature	15 mmHg	[13,137]

Table 15.3 Baseline values for blood pressures in the retina microcirculation model.

Symbol	Description	Value	Source
$p_{LA,b}$	blood pressure in each large arteriole	36.85 mmHg	Eq. (17.43a)
$p_{SA,b}$	blood pressure in each small arteriole	28.73 mmHg	Eq. (17.43a)
$p_{SV,b}$	blood pressure in each small venule	17.56 mmHg	Eq. (17.43a)
$p_{LV,b}$	blood pressure in each large venule	15.71 mmHg	Eq. (17.43a)

Table 15.3 contains the baseline values of the pressure in each compartment of the electric equivalent network in Fig. 15.10. These values are the solution of the linear algebraic system arising from setting $\frac{d\mathbf{P}(t)}{dt} = \underline{\mathbf{0}}$ in (15.72a).

Table 15.4 Parameter values for the various compartments in the representative segment model of the retina.

Symbol	Description	Value					Source
		$j = LA$	SA	CAP	SV	LV	
n_j	number of vessels	4	40	187,890	40	4	[13]
L_j	vessel length [cm]	0.73	0.52	0.067	0.52	0.73	[13]
μ_j	blood viscosity [cP]	2.28	2.06	10.01	2.09	2.44	[13]
D_{0j}	vessel diameter [μm]	105	47.2	6.0	68.5	154.9	[13]
σ_j	distensibility [mmHg^{-1}]	$34.12 \cdot 10^{-4}$	$34.12 \cdot 10^{-4}$	0	$27.29 \cdot 10^{-3}$	$27.29 \cdot 10^{-3}$	[137,184]

Table 15.4 contains the values of the parameters of each compartment in the equivalent electric representation of Fig. 15.10, as determined in [13,137].

The numerical simulations are performed by running the `Matlab` script 28.2.2 and using the values of model parameters reported in Tables 15.2, 15.3, and 15.4. The value of the initial condition for each nodal pressure is $p^0_{LA} = 33.698$ mmHg, $p^0_{SA} = 23.76$ mmHg, $p^0_{SV} = 18.69$ mmHg, and $p^0_{LV} = 16.4$ mmHg. These values can be regarded as a perturbation of the baseline values reported in Table 15.3.

Fig. 15.11 and Fig. 15.12 illustrate the results of the simulation of the pressure for the several retina compartments, as computed with the differential-algebraic model (15.72). Graphs are obtained by keeping the input pressure fixed at $p_{in} = p_{in,b}$, where $p_{in,b} = 40$ mmHg, and by setting the output pressure p_{out} equal to $\Gamma p_{out,b}$, where $p_{out,b} = 15$ mmHg and Γ takes the values 0.5, 1, 2, and 3.

In all reported panels of Fig. 15.11, each black dashed line is the steady-state value of the corresponding considered variable. The steady-state values are the solutions of Eqs. (15.72) having set $\frac{d\mathbf{P}(t)}{dt} = \underline{\mathbf{0}}$. Similarly, the steady-state values for the total flow rates are obtained by replacing the steady-state value of each nodal pressure in Eq. (15.77b).

The analysis of model predictions indicates the following:

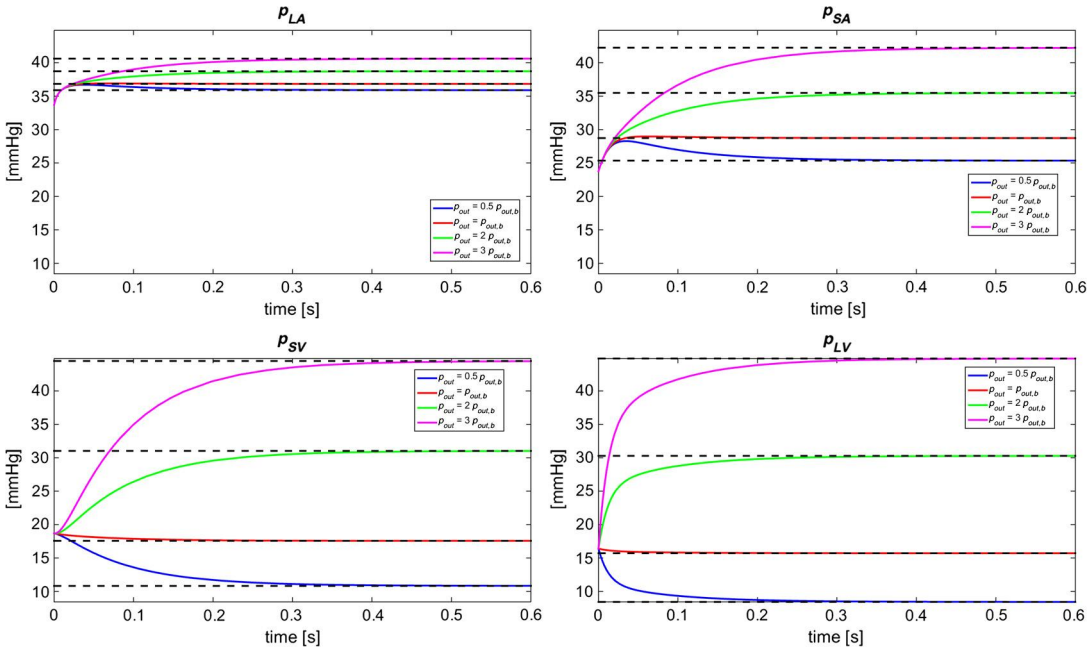

FIGURE 15.11

Time evolution of nodal pressures as a function of the output pressure $p_{out} = \Gamma p_{out,b}$, where $\Gamma = 0.5, 1, 2, 3$. Top row: p_{LA} (left panel), p_{SA} (right panel). Bottom row: p_{SV} (left panel), p_{LV} (right panel). For each plotted pressure, the dashed black line represents the corresponding steady-state value. The same scale has been used on the y axis for all four reported panels.

- In all simulated cases, each electric variable tends to the corresponding steady-state value as time is large enough. This is consistent with the biophysical evidence that the eigenvalues of $-(\underline{\underline{\mathbf{CY}}})^{-1}$ are negative and equal to -330.2913, -85.3632, -79.7748, and -11.5633, so that the lumped electric equivalent circuit of Fig. 15.10 is *asymptotically stable* (see Property 24.1 and Section 3.5.2.3).
- The nodal values of the pressures in the venule compartments experience a small variation if $\Gamma \leq 1$ and a larger variation when Γ increases. In particular, this trend is amplified in the case where $\Gamma = 3$. These results correspond to the inversion of blood flow, which moves from right to left in the electric network, because p_{out} is larger than p_{in}.
- Correspondingly, the total flow rate in the large venule compartment is negative for $\Gamma > 1$ and experiences a much larger variation (in absolute value) than in the other compartments during the transient phase of system network dynamics.

In conclusion, model predictions show that a perturbation of the initial conditions in the retina microcirculation with respect to baseline conditions may give rise to a significant change in the dynamics of the biophysical system. Moreover, model results indicate that the value of the output system pressure may have a relevant impact on the hemodynamic response of the retina, which, under extreme conditions, may even experience an inversion of blood flow. In these conditions, the model predicts a

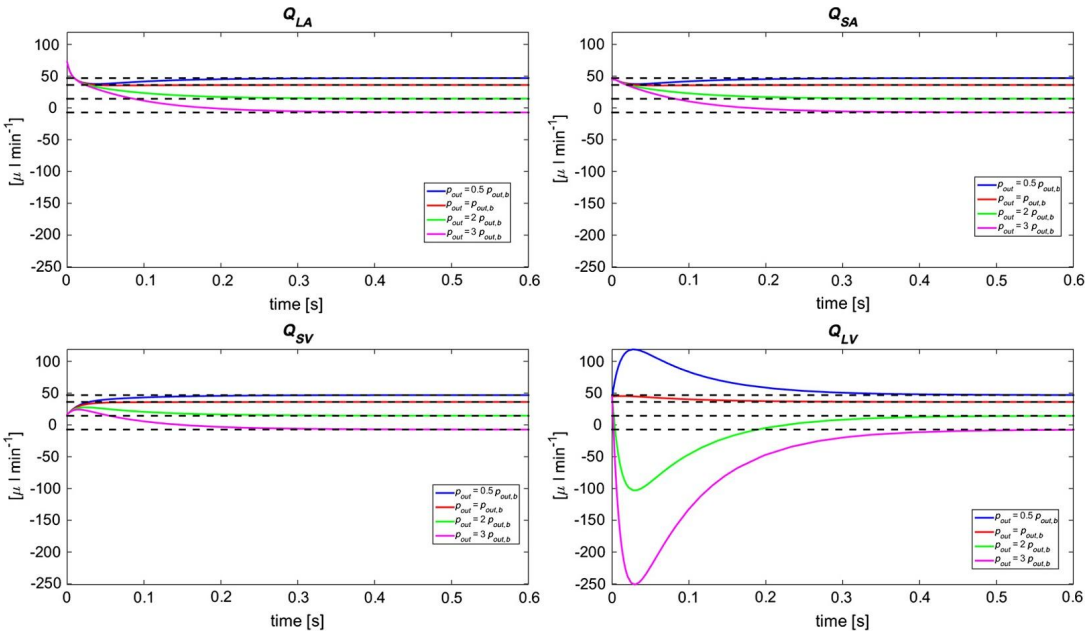

FIGURE 15.12

Time evolution of total flow rates as a function of the output pressure $p_{out} = \Gamma p_{out,b}$, where $\Gamma = 0.5, 1, 2, 3$. Top row: Q_{LA} (left panel), Q_{SA} (right panel). Bottom row: Q_{SV} (left panel), Q_{LV} (right panel). For each plotted flow rate, the dashed black line represents the corresponding steady-state value. The same scale has been used on the y axis for all four reported panels.

significant increase of the pressure in the venule compartment and, as a consequence, an increase in the total blood flow rate. These predictions may help interpret the cause–effect mechanisms underlying pathologies in the retina related to the connection between elevated pressure drop in the venules and venule collapsibility (see Section 15.6).

This page intentionally left blank